

- (3) McCammon, J. A. *Science* **1987**, 238, 486.
- (4) Go, N. *Annu. Rev. Biophys. Bioeng.* **1983**, 12, 183.
- (5) Metropolis, N. et al. *J. Chem. Phys.* **1953**, 21, 1087. Rapa-
port, D. C.; Scheraga, H. A. *Macromolecules* **1981**, 14, 238.
Alder, B. J.; Wainwright, T. J. *J. Chem. Phys.* **1959**, 31, 459.
McCammon, J. A.; Gelin, B. R.; Karplus, M. *Nature* **1977**,
267, 585.
- (6) Gibson, K. D.; Scheraga, H. A. *Physiol. Chem. Phys.* **1969**, 1,
109.
- (7) Gibson, K. D.; Scheraga, H. A. *J. Comp. Chem.* **1987**, 8, 826.
- (8) Vasquez, M.; Scheraga, H. A. *Biopolymers* **1985**, 24, 1437.
- (9) Levitt, M. *J. Mol. Biol.* **1983**, 170, 723.
- (10) Go, N.; Scheraga, H. A. *J. Chem. Phys.* **1969**, 51, 4751.
- (11) Hagler, A. T.; Stern, P. S.; Sharon, R.; Becker, J. M.; Naidler,
F. *J. Am. Chem. Soc.* **1979**, 101, 6842.
- (12) Karplus, M.; Kushick, J. N. *Macromolecules* **1981**, 14, 325.
- (13) Levy, R.; Karplus, M. *Proc. Natl. Acad. Sci.* **1982**, 79, 1346.
- (14) Meirovitch, H.; Vasquez, M.; Scheraga, H. A. *Biopolymers*
1987, 26, 651.
- (15) Paine, G. H.; Scheraga, H. A. *Biopolymers* **1985**, 24, 1391.
- (16) Scheraga, H. A.; Paine, G. H. *Ann. N.Y. Acad. Sci.* **1986**, 482,
60. Paine, G. H.; Scheraga, H. A. *Biopolymers* **1986**, 25, 1547;
1987, 26, 1125.
- (17) Lepage, G. P. *J. Comp. Phys.* **1978**, 27, 192.
- (18) Meirovitch, H.; Vasquez, M.; Scheraga, H. A. *Biopolymers*
1988, 27, 1189.
- (19) See, for example: Hansen, J. P.; McDonald, I. R. In *Theory of*
Simple Liquids; Academic Press: New York, 1976.
- (20) See, for example: Press, W. H.; Flannery, B. P.; Teukolsky, S.
A.; Vetterling, W. T. In *Numerical Recipes*; Cambridge Uni-
versity Press: 1986.
- (21) Mezei, M.; Swaminathan, S.; Beveridge, D. L. *J. Am. Chem.*
Soc. **1978**, 100.
- (22) Jorgensen, W. L.; Ravimohan, C. *J. Chem. Phys.* **1985**, 83, 3050.
- (23) The authors thank an anonymous referee for pointing out this
potential limitation.
- (24) DISCOVER is a molecular dynamics, molecular mechanics simu-
lation package of BIOSYM Technologies, INC., San Diego, CA.
- (25) Hoover, W. G.; Hindmarsh, A. C.; Holian, B. L. *J. Chem.*
Phys. **1972**, 57, 1980.
- (26) Li, Z.; Scheraga, H. A. *J. Phys. Chem.* **1988**, 92, 2633.
- (27) Yoon, B.-J.; Scheraga, H. A., preprint.
- (28) Momany, F. A.; McGuire, R. F.; Burgess, A. W.; Scheraga, H.
A. *J. Phys. Chem.* **1975**, 79, 2361. Nemethy, G.; Pottle, M. S.;
Scheraga, H. A. *J. Phys. Chem.* **1983**, 87, 1883. Sippl, M. J.;
Nemethy, G.; Scheraga, H. A. *J. Phys. Chem.* **1984**, 88, 6231.
- (29) Dauber-Osguthorpe, P.; Roberts, V. A.; Osguthorpe, D. J.; Wolff,
J.; Genest, M.; Hagler, A. T. *Proteins: Structure, Function,*
and Genetics; **1988**, 4, 31.

¹³C NMR Investigation of Molecular Order in Liquid Crystal Polysiloxanes

H. Oulyadi, F. Lauprêtre,* and L. Monnerie

Laboratoire de Physico-Chimie Structurale et Macromoléculaire, associé au CNRS, 10 rue
Vauquelin, 75231 Paris Cédex 05, France

M. Mauzac, H. Richard, and H. Gasparoux

Centre de Recherche Paul Pascal, Université de Bordeaux I, 33405 Talence Cédex, France.
Received March 9, 1989; Revised Manuscript Received October 13, 1989

ABSTRACT: High-resolution variable-temperature ¹³C NMR experiments have been carried out on a series of side-chain liquid-crystal polysiloxanes. The ¹³C chemical shift dependence on temperature observed in the mesophases is a clear indication that the polysiloxanes orient in the magnetic field. Results have been interpreted in terms of molecular order and local dynamics of the different parts of the molecule: spacer, mesogenic core, and terminal group of the side chain. It has been shown that the spacer and the terminal group do not have the same influence on the order parameter associated with the mesogenic core. The apparent variations of the order parameter along the side chain reflect the existence of several motional processes occurring in the oriented mesophase. Among them are the trans-gauche conformational changes in the spacer, the internal rotation of the phenyl rings about their symmetry axis, the motion of the COO plane associated with the β₂ transition of polysiloxanes, and the overall rotation of the whole side group about its molecular axis.

Side-chain liquid-crystal polymers are interesting materials which combine the properties of polymers and those of liquid crystals of low molecular weight. A deeper understanding of the behavior of these compounds requires the investigation of molecular order and dynamics in the different phases. Some studies have already been performed using X-ray,¹ small-angle neutron scattering,^{2,3} dielectric relaxation,⁴⁻¹¹ and ²H NMR.¹²⁻¹⁴ High-resolution ¹³C NMR is also a powerful technique which has proven to be useful in the determination of order and dynamics of small liquid-crystal molecules.¹⁵⁻¹⁷ The natural carbon-13 abundance makes it unnecessary to do any kind of labeling, and the selectivity of the technique allows the observation of each magnetically inequivalent

carbon independently. In this paper we report a high-resolution ¹³C NMR investigation of molecular order of a series of side-chain liquid-crystal polysiloxanes. Some results concerning the dynamics of these systems will also be described.

Experimental Section

The polysiloxanes (P_{n,m}) of the general formula

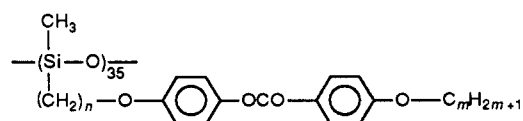


Table I
Glass Transition Temperatures, T_g , Melting Temperatures, T_m , and Phase Transition Temperatures ($^{\circ}\text{C}$) of the $P_{n,m}$ Polysiloxanes¹

n	m	T_g	T_m	$S_B \rightarrow$	$S_C \rightarrow$	$S_A \rightarrow$	$N \rightarrow \text{iso}$	polymer index
3	1	15				119		$P_{3,1}$
4	1	7				74	104	$P_{4,1}$
	2	17				113	127	$P_{4,2}$
	4	31	75			141		$P_{4,4}$
	8			55		133		$P_{4,8}$
5	1	4	71			122		$P_{5,1}$
6	1	-4				109		$P_{6,1}$
11	1	24	56		60	134		$P_{11,1}$

were synthesized at CRPP.¹ The number of monomer units per chain is 35. The nature and temperature of the different phase transitions are listed in Table I as a function of m and n .

High-resolution ^{13}C NMR experiments were conducted at 75 MHz with a BRUKER CXP 300 spectrometer, with quadrature detection and a single rf coil, which was double-tuned for both ^{13}C and ^1H NMR. Experiments were performed either on static samples or on magic-angle spinning samples. Spinning experiments were done with Al_2O_3 rotors at spinning speeds of 4 kHz. The pulse sequences consisted either of a single carbon pulse followed by proton dipolar decoupling or of a cross-polarization proton dipolar decoupling sequence. The matched spin-lock cross-polarization transfers were carried out with ^{13}C and ^1H magnetic field strengths of 64 kHz. Spin-temperature inversion techniques allowed the minimization of base-line noise and roll.¹⁸ Flip-back¹⁹ was also used to shorten the delay between two successive cross-polarization sequences.

Results and Discussion

Among the polysiloxanes whose characteristics are listed in Table I, most of them present only one smectic A mesomorphic phase. However, the $P_{4,1}$ and $P_{4,2}$ samples have both nematic and smectic A phases. We will first focus on the results obtained from the smectic A phases only, and, as an example, we will describe the behavior of the $P_{5,1}$ polymer. Then, we will examine the case of the polysiloxanes in their nematic phase.

I. Smectic A Liquid-Crystal Polysiloxanes. I.1. $P_{5,1}$. Orientational Effects in the Magnetic Field. The proton dipolar decoupled ^{13}C NMR spectrum of a static sample of $P_{5,1}$ at high temperature (129°C) and the ^{13}C NMR spectrum at 62°C of an unoriented sample of $P_{5,1}$ recorded at 75 MHz under conditions of magic angle spinning, proton dipolar decoupling, and cross-polarization are shown in parts a and b of Figure 1. Both spectra present the same number of well-resolved lines with very similar chemical shifts. The $P_{5,1}$ sample at 129°C is in its isotropic phase, and the molecular motions are fast enough to average the chemical shift anisotropies. Therefore, only the traces of the ^{13}C chemical shift tensors are observed in Figure 1a. At 62°C , in the smectic A phase of $P_{5,1}$, the use of rapid magic angle sample spinning and proton dipolar decoupling, which are the well-known techniques for high-resolution solid-state ^{13}C NMR,²⁰ allows the observation of the isotropic part of the chemical shift tensors in the unoriented powder. In the case of the aromatic carbons, the individual line assignment is based on empirical substituent additivity effects in benzene derivatives.²¹ Substituent additivity effects in linear alkanes²¹ have been used to assign the aliphatic lines. The whole line assignment is summarized in the spectrum represented in Figure 1a.

Proton-decoupled 75-MHz ^{13}C NMR spectra of a static sample of $P_{5,1}$ at different temperatures, T , are shown in Figure 2. They have been obtained after cooling the $P_{5,1}$ polysiloxane slowly from the isotropic state to the smec-

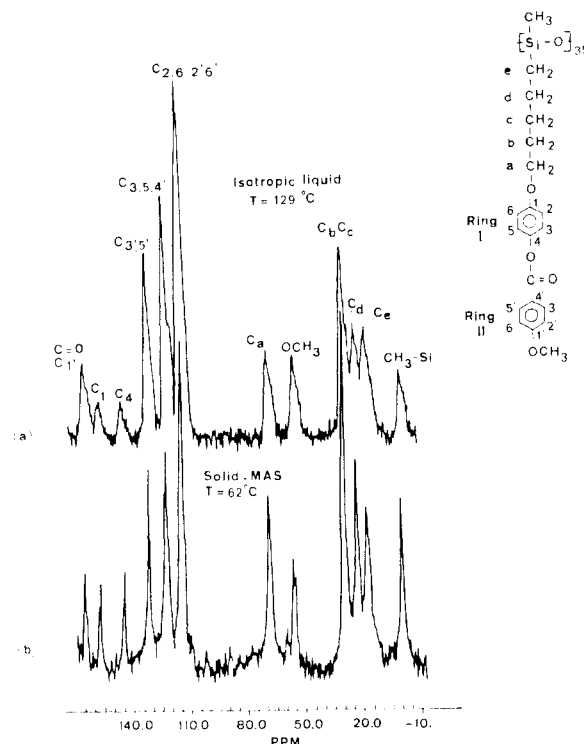


Figure 1. (a) 75-MHz proton dipolar decoupled ^{13}C NMR spectrum of a static sample of $P_{5,1}$ at 129°C . (b) 75-MHz ^{13}C NMR spectrum of an unoriented sample of $P_{5,1}$ at 62°C obtained by using magic angle spinning, proton dipolar decoupling, and cross-polarization.

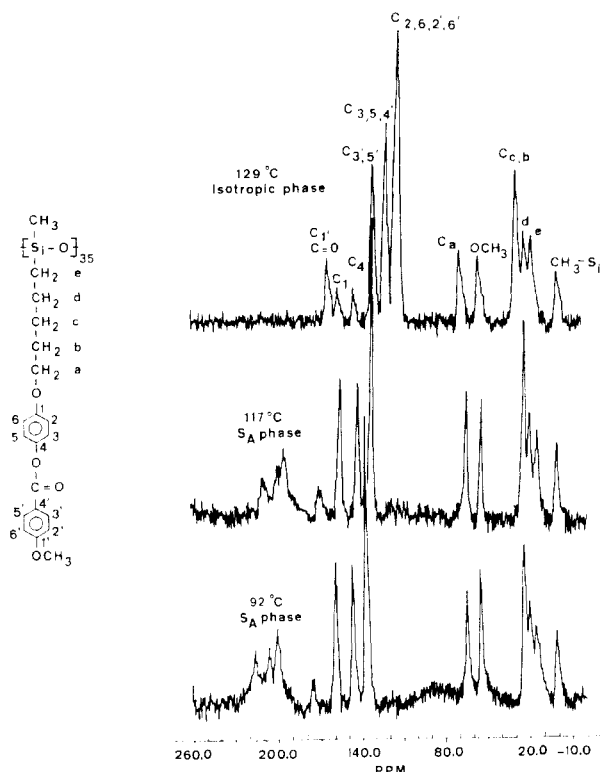


Figure 2. 75-MHz proton dipolar decoupled ^{13}C NMR spectrum of a static sample of $P_{5,1}$ recorded at decreasing temperatures.

tic A (S_A) phase in the strong magnetic field (7 T) of the NMR spectrometer. The spectrum recorded at a temperature of 117°C , just below the S_A -iso transition temperature, T_{iso} , has narrow lines that are strongly shifted with respect to those observed in the isotropic phase. Aromatic and carboxyl carbon lines are shifted to lower fields

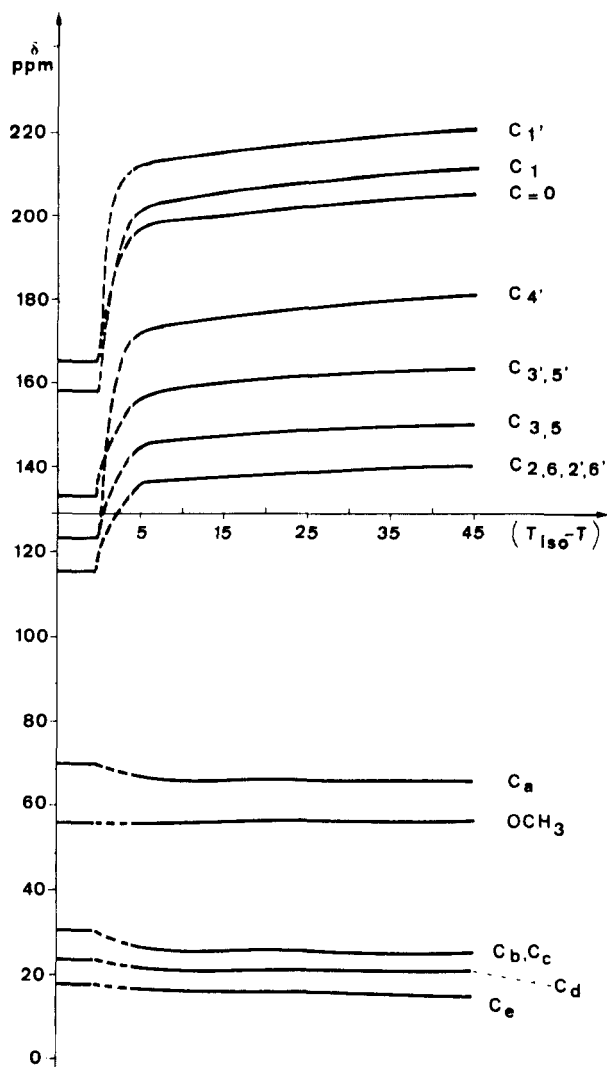


Figure 3. Chemical shift dependence of the carbons of a static sample of $P_{5,1}$ on decreasing temperature. Dots are given only as an indication in order to follow the chemical shift variation of each line.

while methylene carbon lines are shifted to higher fields. The lines remain narrow, but the chemical shift variations increase on decreasing temperature and then tend to limiting values. Only the chemical shift of the methoxy line is independent of temperature. Complete line assignment in the smectic A phase was first obtained both by taking into account the line intensities and by assuming a quasi-continuous chemical shift variation from the isotropic phase spectrum. It was further corroborated by calculations of the order parameter reported in the following sections. The chemical shifts of the various lines are plotted in Figure 3 as a function of $(T_{180} - T)$. Chemical shifts are constant in the isotropic phase, they suddenly vary at the S_A -iso transition, and then they tend monotonically to finite values in the S_A phase as the temperature decreases.

The observation of narrow lines with chemical shifts that differ from the isotropic values indicates that the polysiloxane molecules in the smectic A phase are oriented in the magnetic field. Similar orientation phenomena in a large magnetic field have been reported for a number of liquid-crystal polymers such as side-chain liquid-crystal polyacrylates¹² and main-chain liquid-crystal polyester-ethers.²²

Mesogenic Core Carbons. Aromatic Carbons of Ring I. In uniaxial phases, the average direction of ori-

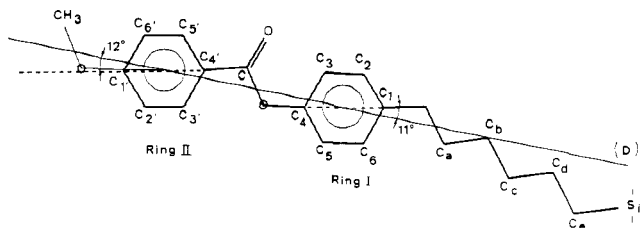


Figure 4. Geometry of the side chain of $P_{5,1}$ ²³ and definition of the molecular axis D .

entation of the molecular long axes for the molecules defines the director. The reference frame (x_4, y_4, z_4) associated with the mesophase is chosen so that the z_4 axis lies along the director. If the molecules are taken to be rodlike, the degree of parallel order of the individual molecular long axis, z_2 , is described by a single orientational order parameter $S_{z_2z_4}$. Strictly speaking, liquid-crystal molecules are not axially symmetric but have an oblong structure leading to a bladelike shape in such a way that the two coordinate axes of the molecular frame normal to the long axis may have different order parameters with respect to the director. The orientational order of the molecule must then be described by a tensor with three principal values, $S_{x_2x_4}$, $S_{y_2y_4}$, and $S_{z_2z_4}$. As the tensor is traceless, the orientational order and its symmetry are completely described by the two parameters $S_{z_2z_4}$ and the difference $S_{x_2x_4} - S_{y_2y_4}$. However, as the latter term is usually small in uniaxial phases of small-molecule liquid crystals, the simplifying assumption of rodlike behavior for such compounds is often appropriate.

In the following, we will consider, as a first approximation, that the mesogenic cores in the liquid-crystal polymers under study are rodlike. The consistency of the results will serve as a test for the validity of this assumption. Therefore, in order to interpret the chemical shift variations in terms of polymer orientation, we have used the classical description normally employed for small-molecule smectic A or nematic liquid crystals.^{15,16} Specifically, we assumed that the bond angles of the mesogenic group shown in Figure 4 are the same as those determined for phenyl benzoate in the crystalline state.²³ Then a molecular long axis, D , which passes through the centers of the two phenyl rings I and II (as numbered in Figure 4) was defined. The entire side chain—spacer, mesogenic group, and terminal part—has been assumed to rotate rapidly as a whole about this molecular axis in the smectic A phase. Under these conditions of rapid rotation, the chemical shift tensors are motionally averaged and present principal elements, σ_{\parallel} and σ_{\perp} , parallel and perpendicular to the rotation axis, D . The observed chemical shifts, σ , are given by

$$\sigma = \sigma_{\text{iso}} + (2/3)S(\sigma_{\parallel} - \sigma_{\perp}) \quad (1)$$

where σ_{iso} is the chemical shift in the isotropic phase and S is the order parameter associated with the molecular axis D and is defined as

$$S = \langle 3 \cos^2 \theta - 1 \rangle / 2 \quad (2)$$

where θ describes the orientation of the long molecular axis D with respect to the applied static magnetic field, and $\langle \rangle$ is a thermal average.

In the simple case of a rapid rotation about the molecular axis, σ_{\parallel} and σ_{\perp} are given by the formulas

$$\begin{aligned} \sigma_{\parallel} &= \sin^2 \beta (\cos^2 \alpha) \sigma_{11} + \sin^2 \beta (\sin^2 \alpha) \sigma_{22} + (\cos^2 \beta) \sigma_{33} \\ \sigma_{\perp} &= (\sigma_{11} + \sigma_{22} + \sigma_{33} - \sigma_{\parallel}) / 2 \end{aligned} \quad (3)$$

where α and β are the two first EULER angles taken as

Table II
Shielding Tensor Elements Used for the Interpretation of Data Relative to Aromatic and Carboxyl Carbons of the Mesogenic Group

carbon	σ_{11}	σ_{22}	σ_{33}	$\sigma_{\parallel} - \sigma_{\perp}$	ref
C ₁	-230	-162	-74	-108.6	25
C _{2,6}	-198	-136	-23	-50.4	25
C _{3,5}	-193	-134	-12	-55.2	25
C _{1'}	-237.7	-166.7	-67.7	-118.15	26
C _{4'}	-221.7	-155.7	30.7	-122.3	27
C _{3',5'}	-226	-153	-15	-61.2	26
C _{2',6'}	-184.7	-131.7	-18.7	-50.8	26
C=O	-250	-122	-122	-80.7	28

defined in ref 24. They describe the orientation of the rotation axis in the principal axes (σ_{11} , σ_{22} , σ_{33}) system.

For aromatic carbons, the general features of the principal values of the chemical shift tensor have been determined from single-crystal studies.²⁵⁻²⁷ The elements of the ¹³C chemical shift tensors for the model compounds used in this study are listed in Table II. For aromatic nuclei, the least shielded element is in the aromatic plane pointing radially out from the ring, and the most shielded one is perpendicular to the plane. Thus, in the case of side chains preferentially aligned with their molecular director *D* along the static magnetic field, a downfield shift of the aromatic lines is expected, and this shift is, in fact, observed, as shown in Figure 2.

Moreover, in the spectra recorded in the mesophase and shown in Figure 2, only one line is observed for each pair of aromatic carbons in an ortho position. The magnetic equivalence of such carbon pairs indicates that the two phenyl rings of the mesogenic core perform at least 180° ring flips. Assuming that the two phenyl rings rotate rapidly about their para axis, the chemical shifts of the aromatic carbons can be written for the para carbons as¹⁵

$$\sigma_{\parallel} = \sigma_{11} \cos^2 \Phi + \sigma_{22} \sin^2 \Phi$$

$$\sigma_{\perp} = 1/2(\sigma_{11} \sin^2 \Phi + \sigma_{22} \cos^2 \Phi + \sigma_{33}) \quad (4)$$

and for the ortho and meta carbons

$$\sigma_{\parallel} = 1/4(1 + 2 \sin^2 \Phi)\sigma_{11} + 1/4(1 + 2 \cos^2 \Phi)\sigma_{22}$$

$$\sigma_{\perp} = 1/2[1/4(1 + 2 \cos^2 \Phi)\sigma_{11} + 1/4(1 + 2 \sin^2 \Phi)\sigma_{22} + \sigma_{33}] \quad (5)$$

Φ is the angle between the para axis of each phenyl ring and the molecular axis *D*. According to geometrical data on phenyl benzoate²³ reported in Figure 4, Φ is equal to 11° and 12° for rings I and II, respectively.

From the chemical shift variations of the different aromatic carbons of ring I shown in Figure 3 and reported values of chemical shift principal values listed in Table II, values of *S* have been calculated using formulas 1, 4, and 5. They are reported in Figure 5. The bar corresponds to the different values of *S* calculated from all the aromatic carbons of ring I. It must be noted that the dispersion is very small.

Carboxyl Carbon and Aromatic Carbons of Ring II. The same type of calculation has been carried out for the carboxyl carbon of the mesogenic core and for the aromatic carbons of ring II.

The chemical shift tensor elements of the carboxyl carbon have been taken from a recent poly(ethylene terephthalate) ¹³C NMR study.²⁸ They are listed in Table II.

As discussed above, it has been assumed in the following that the side chain reorients as a whole about the

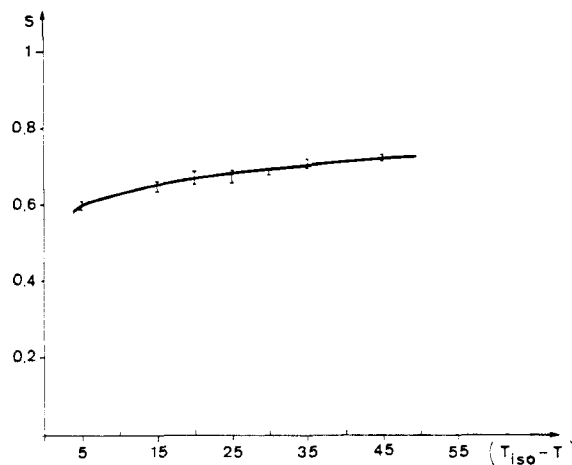


Figure 5. Dependence of the order parameter *S* of P_{5,1}, calculated from the chemical shift variations of the aromatic carbons of ring I, as a function of temperature.

molecular axis *D* and that the two phenyl rings are in rapid rotation about their symmetry axis.

With the additional assumption that the COO group is in the fixed geometry shown in Figure 4, one observes a large dispersion in the values of *S* calculated from the chemical shift variation of the carboxyl and aromatic carbons of ring II. This result is in contrast with the results obtained from the ring I carbons. Moreover, the relatively small value of *S* calculated from the carboxyl carbon data can be interpreted in terms of internal motion of the COO group about the O-C_{arom} bond. Indeed, the existence of a specific motion of the carboxyl group in liquid-crystal polysiloxanes, as well as in polyacrylates, has already been pointed out by dielectric relaxation experiments.^{4,10,11} It is known to correspond to the β_2 relaxation process.

In order to account for this specific motion of the COO group, it has been assumed that, besides the motional processes already considered (side-chain reorientation about *D* and phenyl ring rotations), the COO plane jumps rapidly between two positions, α and $-\alpha$ or α and $\pi - \alpha$, where α is the angle between the rest and jump position of the COO plane. Under these conditions, one calculates from the carboxyl carbon data a value of *S*, which is equal to those reported in Figure 5 when α is of the order of 90°, in the case of fast jumps between α and $-\alpha$, and a value of α in the range 0°–40° for jumps between α and $\pi - \alpha$. The latter result is in very good agreement with the interpretation of ¹³C chemical shift anisotropy of the carboxyl carbon of benzenhexa-*n*-hexanoate in its phase I reported in ref 29.

Results obtained for the aromatic carbons of ring II can also be interpreted by taking into account this additional motion of the COO plane. As for the carboxyl carbon, good agreement is obtained between the different sets of data for large-amplitude jumps of the COO plane.

Within the above description of local motions of the mesogenic cores, values of *S* deduced from the chemical shift variations observed for the carboxyl carbon and aromatic carbons of phenyl ring II are equal to those calculated from the behavior of the aromatic carbon lines of phenyl ring I and reported in Figure 5.

Aliphatic Carbons of the Spacer and Terminal Group. Regarding the terminal group of the side chain, the line at 55.5 ppm, which corresponds to the methoxy carbon, does not change from the isotropic state to the mesophase. This result indicates that the average angle between the O-CH₃ axis and the long molecular axis *D*

Table III
Shielding Tensor Elements Used for the Interpretation of Data Relative to the Aliphatic Carbons of the Spacer

¹³ C	ref	σ_{11}	σ_{22}	σ_{33}	$\sigma_{ } - \sigma_{\perp}$ ^a		
					(a)	(b)	(c)
C _a	26	-91	-78	-38	8.38	0.69	
C _b	30	-38	-31	-16	16.52	5.88	-7.18
C _c	30	-38	-31	-16	16.52	-7.88	5.88
C _d	26	-31	-21	-15	10.23	5.17	-4.3

^aEULER angles (deg) (α, β) defining the orientation of the molecular axis *D* in the principal axes system of carbons C_b, C_c, and C_d: (a) (α, β) = (90; 17.4) (trans conformation of the spacer); (b) (α, β) = (68.4; 46.6); (c) (α, β) = (44.2; 75.4). See Table V for the relation between the conformational sequences and the values of the EULER angles.

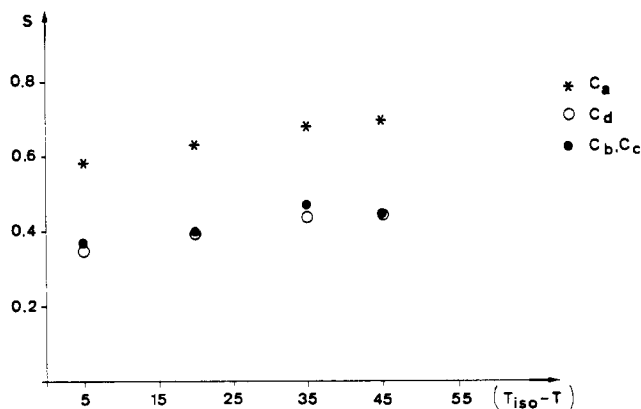


Figure 6. Dependence of the order parameter *S* of P_{5,1}, calculated from the chemical shift variations of the aliphatic carbons of the spacer assuming a trans conformation of the side chain, as a function of temperature.

is close to the magic angle. Identical results have been found by Pines and Chang¹⁵ for the methoxy group of the (*p*-methoxybenzylidene)-*p*'-*n*-butylaniline (MBBA) molecule.

Principal elements of the shielding tensors of methylene carbons have been determined by Vanderhart in the case of *n*-eicosane³⁰ and by Hohener for alkoxy derivatives of *p*-benzoic acid in an unpublished work cited in ref 26. Among the different tensors of methylenic carbons determined by these authors, we have chosen those whose trace is the closest to the experimental value determined in the isotropic phase of our polysiloxanes. Their values are indicated in Table III. The most shielded vector is parallel to the chain axis; the least shielded one is parallel to the proton-proton vector.³⁰ The most shielded element of the O-CH₂ carbon has been taken parallel to the O-C bond according to ref 31.

Assuming that the ether linkage of the alkoxy spacer is held fixed in the plane of the adjacent aromatic ring I and that all the spacer bonds are in a trans conformation, calculation of *S* using formulas 1 and 3 and data obtained on aliphatic carbons and shown in Figure 3 yields the results reported in Figure 6. The O-CH₂ carbon next to the mesogenic core leads to values of *S* that are identical with those deduced from the mesogenic group data. For the other spacer carbons, a much weaker order parameter is thus calculated. This result implies that the above assumption of a fixed trans conformation of the whole spacer is not correct. The apparent decrease of *S* can be assigned to a fast dynamic exchange between trans, gauche(+), and gauche(-) conformations, as already observed using ²H NMR on a number of small-molecule liquid crystals³² and some main-chain²² and side-chain¹² liquid-crystal polymers.

Table IV
Matrix of Statistical Weights for the Spacer Bonds

ϕ_i	ϕ_{i-1}		
	trans	gauche(+)	gauche(-)
trans	$1 - P_i$	1	1
gauche(+)	$P_i/2$	0	0
gauche(-)	$P_i/2$	0	0

Table V
Probabilities of the Conformational Sequences Encountered in the Spacer and EULER Angles Defining the Orientation of the Molecular Axis *D* in the Principal Axes Systems of Carbons C_b, C_c, and C_d

sequence	probability	EULER angles (α, β)		
		C _b	C _c	C _d
tttt	$(1 - P_b)(1 - P_c)(1 - P_d)$	90; 17.4	90; 17.4	90; 17.4
tttg ⁺	$(1 - P_b)(1 - P_c)P_d/2$	90; 17.4	90; 17.4	68.4; 46.6
tttg ⁻	$(1 - P_b)(1 - P_c)P_d/2$	90; 17.4	90; 17.4	68.4; 46.6
ttgt ⁺	$(1 - P_b)P_c/2$	90; 17.4	44.2; 74.5	44.2; 74.5
ttgt ⁻	$(1 - P_b)P_c/2$	90; 17.4	44.2; 74.5	44.2; 74.5
tg ⁺ tt	$P_b(1 - P_d)/2$	68.4; 46.6	68.4; 46.6	68.4; 46.6
tg ⁻ tt	$P_b(1 - P_d)/2$	68.4; 46.6	68.4; 46.6	68.4; 46.6
tg ⁺ tg ⁺	$(P_b/2)(P_d/2)$	68.4; 46.6	68.4; 46.6	68.4; 46.6
tg ⁺ tg ⁻	$(P_b/2)(P_d/2)$	68.4; 46.6	68.4; 46.6	90; 17.4
tg ⁻ tg ⁺	$(P_b/2)(P_d/2)$	68.4; 46.6	68.4; 46.6	90; 17.4
tg ⁻ tg ⁻	$(P_b/2)(P_d/2)$	68.4; 46.6	68.4; 46.6	68.4; 46.6

In order to determine the expression of the matrix of the statistical weights at the sites of the b, c, and d carbons, we have assumed that the conformational jumps occur between trans, gauche(+), and gauche(-) positions and that the probability for two successive gauche conformations is very low. This last assumption is in agreement with the results of conformational energy calculations carried out by Samulski and Toriumi³³ on nematogenic molecules with alkoxy groups. If we then assume that the probability $P_i/2$ for a trans-gauche(+) sequence at the site of the *i*th carbon is equal to the probability for a trans-gauche(-) one, the matrix of statistical weights can be expressed as shown in Table IV.

The probabilities of the different conformational sequences that can be encountered in the spacer are given in Table V, together with the EULER angles characterizing the orientation of the chemical shift tensor axes with respect to the molecular axis *D*, for each carbon C_b, C_c, and C_d of the spacer.

The anisotropies of the chemical shift tensors of the spacer carbons averaged by the rapid rotation about the molecular axis are given in Table III.

Assuming a fast exchange between the gauche and trans conformations, the values of the probabilities, P_i , are given by the equations

$$\begin{aligned}
 (1 - P_b)16.5 + P_b5.9 &= (3(\sigma_m - \sigma_{iso})/2S)C_b \\
 (1 - P_b)(1 - P_c)16.5 + (1 - P_b)P_c(-7.4) + P_b5.9 &= \\
 &= (3(\sigma_m - \sigma_{iso})/2S)C_c \\
 [P_bP_d/2 + (1 - P_b)(1 - P_c)(1 - P_d)]10.2 + [(1 - P_b)(1 - P_c)P_d + P_b(1 - P_d/2)]5.2 + (1 - P_b)P_c(4.5) &= \\
 &= (3(\sigma_m - \sigma_{iso})/2S)C_d
 \end{aligned}$$

where σ_m is the measured value of the chemical shift in the smectic phase and σ_{iso} is the chemical shift in the isotropic phase of the bulk polymer.

In the case of the P_{5,1} polysiloxane, the application of the above formulas to the experimental results shown in Figure 3 leads to

$$P_b = 0.6 \text{ and } P_c = 0$$

for the limiting values of *S* at low temperature. The accu-

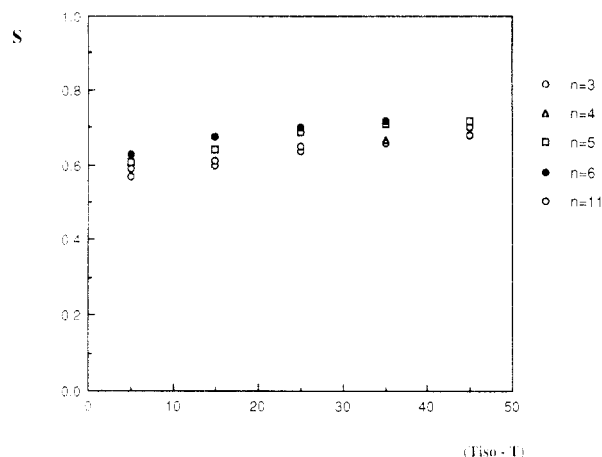


Figure 7. Dependence of the order parameter S , calculated from the chemical shift variations of the aromatic carbons of ring I, as a function of temperature, in the smectic A phase of the $P_{n,1}$ polysiloxanes.

racy of the experiments is not sufficient to determine P_d . The proportions of the different sequences are

$$(tttt + ttg^+ + ttg^-) = 0.4$$

$$(ttg^+t + ttg^-t) = 0$$

$$(tg^+tt + tg^-tt + tg^+tg^+ + tg^+tg^- + tg^-tg^+ + tg^-tg^-) = 0.6$$

It must be noticed that the $(\sigma_m - \sigma_{iso})/2S$ ratio is independent of temperature, which implies that these proportions, which have been evaluated from the low-temperature experiments, are constant within the whole smectic phase. The only variable that is a function of temperature is the value of the order parameter.

It is of interest to compare our results to the conclusions of the conformational energy calculations carried out by Samulski and Toriumi³³ on nematogens with alkoxy chains. In these compounds, the calculated probabilities for $txxx$, $(ttt + ttg)$, $ttgt$, and $(tgtt + tgtg)$ states, where x is either a trans conformation or a gauche(\pm) one, are 100%, 34%, 6%, and 47%, respectively. These results are in reasonable agreement with the NMR results reported above, taking into account the fact that we have neglected the gauche-gauche sequences: the gauche states are excluded at the site of the O-CH₂ bond, which minimizes the interactions between the protons of ring I and the second CH₂ of the spacer. The $tttt$, $ttgt$, ttg , and $tttg$ conformations have a high probability. They correspond to a nearly extended geometry of the spacer, which should favor the molecular arrangement of the side chains.

I.II. Other Smectic A Liquid-Crystal Polysiloxanes. Influence of the Lengths of the Spacer and of the Terminal Group on the Order Parameter. The same NMR experiments have been performed on all the polysiloxanes listed in Table I. For all these compounds, orientational effects in the 7-T magnetic field of the NMR spectrometer have been observed.

In Figure 7 the values of S determined from the chemical shift variations of the aromatic carbons are plotted as a function of temperature for some $P_{n,1}$ polymer systems in their smectic A phase. They all exhibit similar variations as a function of decreasing temperature. The order parameter increases only slightly as a function of the spacer length, and it reaches a limiting value for $n = 6$.

On the contrary, as shown by values of S in Figure 8 for the $P_{4,m}$ polymers, the length of the terminal side group has a stronger influence on the order parameter.

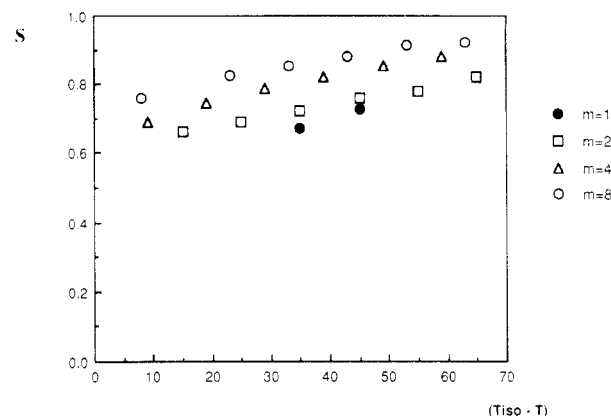


Figure 8. Temperature dependence of the order parameter S , calculated from the chemical shift variations of the aromatic carbons of ring I, in the smectic A phase of the $P_{4,m}$ polysiloxanes.

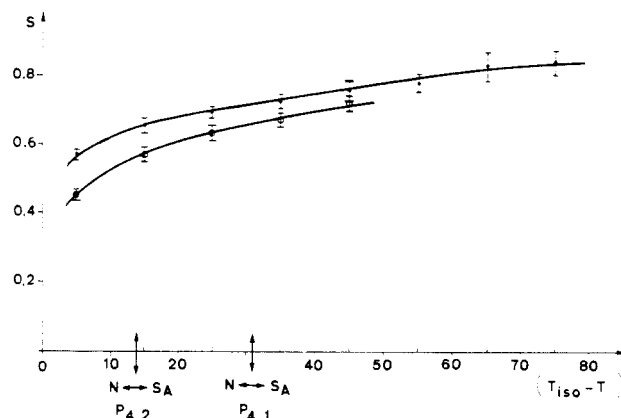


Figure 9. Temperature dependence of the order parameter S , calculated from the chemical shift variations of the aromatic carbons of ring I, in the nematic and smectic A phases of the $P_{4,1}$ (Φ) and $P_{4,2}$ (\bullet) polysiloxanes.

Table VI
Probability of a g^\pm State at Each CH₂ Site in $P_{5,1}$ and $P_{4,1}$

	P_a	P_b	P_c
$P_{5,1}$	0	0.6	0
$P_{4,1}$	0	0.7	

The maximum values are much higher than those obtained on increasing the spacer length. Spacer and terminal groups thus do not affect the mesogenic group equivalently. From the data reported in Figures 7 and 8, it appears that the constraints opposed by the polysiloxane main chain at the spacer extremity do not favor maximum order.

The conformational order of the spacer can only be determined experimentally in systems having short spacers and a methoxy terminal group. In the other polymers, there is an overlap of the numerous aliphatic lines. As an example, values obtained for the $P_{4,1}$ spacer are listed in Table VI. They show the same general features as those observed in $P_{5,1}$.

II. Nematic Liquid-Crystal Polysiloxanes. Among the compounds listed in Table I, the $P_{4,1}$ and $P_{4,2}$ polysiloxanes exhibit a nematic phase. For these polymers too, orientational effects are observed in the 7-T magnetic field of the NMR spectrometer when the samples are cooled slowly from the isotropic phase as described previously. Values of the order parameter calculated from the chemical shift variations of the aromatic carbons of ring I are shown in Figure 9. They are somewhat lower than those obtained in the smectic A phase for a given

$T_{\text{iso}} - T$ difference. However, in the case of these polysiloxanes, which have both nematic and smectic A phases, no discontinuity is observed, within the sensitivity of the experiments, at the nematic-smectic A transition temperature.

Conclusion

This ^{13}C NMR study of side-chain liquid-crystal polysiloxanes has led to a detailed description of molecular order and local motions in the different parts of the molecule: spacer, mesogenic core, and terminal group of the side chain. It has shown the different influence of the spacer and terminal group on the order parameter associated with the mesogenic core. Moreover, apparent variations of the order parameter along the side chain can be interpreted quantitatively in terms of several motional processes occurring simultaneously in the oriented mesophase. Among them are the trans-gauche conformational changes in the spacer, the internal rotation of the phenyl rings about their symmetry axis, the motion of the COO plane associated with the β_2 transition of polysiloxanes, and the overall rotation of the whole side group about its molecular axis.

References and Notes

- Mauzac, M.; Hardouin, F.; Richard, M.; Achard, M. F.; Sigaud, G.; Gasparoux, H. *Eur. Polym. J.* **1986**, *22*, 137.
- Keller, P.; Carvalho, B.; Cotton, J. P.; Lambert, M.; Moussa, F.; Pepy, G. *J. Phys. Lett.* **1985**, *46*, L-1065.
- Moussa, F.; Cotton, J. P.; Hardouin, F.; Keller, P.; Lambert, M.; Pepy, G.; Mauzac, M.; Richard, H. *J. Phys. (Les Ulis, Fr.)* **1987**, *48*, 1079.
- Njeumo, R. Thèse de Docteur-Ingénieur, Lille, France, 1986.
- Attard, G. S. *Mol. Phys.* **1986**, *58*, 1087.
- Araki, K.; Attard, G. S. *Liq. Cryst.* **1986**, *1*, 301.
- Attard, G. S.; Williams, G. *Liq. Cryst.* **1986**, *1*, 253.
- Attard, G. S.; Moura-Ramos, J. J.; Williams, G. *J. Polym. Sci., Polym. Phys. Ed.* **1987**, *25*, 1099.
- Zentel, R.; Strobl, G. R.; Ringsdorf, H. *Macromolecules* **1985**, *18*, 960.
- Parneix, J. P.; Njeumo, R.; Legrand, C.; Le Barny, P.; Dubois, J. C. *Liq. Cryst.* **1987**, *2*, 167.
- Haase, W.; Pranoto, H.; Bormuth, F. J. *Ber. Bunsen-Ges. Phys. Chem.* **1985**, *89*, 1229.
- Boeffel, C.; Hisgen, B.; Pschorn, U.; Ringsdorf, H.; Spiess, H. W. *Isr. J. Chem.* **1983**, *23*, 388.
- Spiess, H. W. *Pure Appl. Chem.* **1985**, *57*, 1617.
- Pschorn, U.; Spiess, H. W.; Hisgen, B.; Ringsdorf, H. *Makromol. Chem.* **1986**, *187*, 2711.
- Pines, A.; Chang, J. J. *Phys. Rev. A* **1974**, *10*, 946.
- Pines, A.; Chang, J. J. *J. Am. Chem. Soc.* **1974**, *96*, 590.
- Rutar, V.; Blinc, R.; Vilfan, M.; Zann, A.; Dubois, J. C. *J. Phys. (Les Ulis, Fr.)* **1982**, *43*, 761.
- Stejskal, E. D.; Schaefer, J. J. *Magn. Reson.* **1975**, *18*, 560.
- Tegenfeldt, J.; Haeberlen, U. *J. Magn. Reson.* **1979**, *36*, 453.
- Schaefer, J.; Stejskal, E. D.; Buchdahl, R. *Macromolecules* **1977**, *10*, 384.
- Wehrli, F.; Wirthlin, T. *Interpretation of Carbon-13 NMR Spectra*; Heyden: London, 1976.
- Mueller, K.; Meier, P.; Kothe, G. *Prog. NMR Spectrosc.* **1985**, *17*, 211.
- Adams, J. M.; Morsi, S. E. *Acta Crystallogr.* **1976**, *B32*, 1345.
- Edmonds, A. R. *Angular Momentum in Quantum Mechanics*, 3rd ed.; Hofstadter, R., Ed.; Princeton University Press: Princeton, NJ, 1974, p 7.
- Maricq, M. M.; Waugh, J. S. *J. Chem. Phys.* **1979**, *70*, 3300.
- Wemmer, D. E.; Pines, A.; Whitehurst, D. D. *Philos. Trans. R. Soc. London* **1981**, *A-300*, 15.
- Tegenfeldt, J.; Feucht, H.; Ruschitzka, G.; Haeberlen, U. *J. Magn. Reson.* **1980**, *39*, 509.
- Harbison, G. S.; Vogt, V. D.; Spiess, H. W. *J. Chem. Phys.* **1987**, *86*, 1206.
- Lifshitz, E.; Goldfarb, D.; Vega, S.; Luz, Z.; Zimmermann, H. *J. Am. Chem. Soc.* **1987**, *109*, 7280.
- Vanderhart, D. L. *J. Chem. Phys.* **1976**, *64*, 830.
- Sergot, P.; Laupretre, F.; Louis, C.; Virlet, J. *Polymer* **1981**, *22*, 1150.
- Hsi, S.; Zimmermann, H.; Luz, Z. *J. Chem. Phys.* **1978**, *69*, 4126.
- Samulski, E. T.; Toriumi, H. *J. Chem. Phys.* **1983**, *79*, 5194.

Diaphragmatic Chemical Polymerization of Pyrrole in the Nafion Film

Tomokazu Iyoda, Akira Ohtani, Kenichi Honda, and Takeo Shimidzu*

Division of Molecular Engineering, Graduate School of Engineering, Kyoto University, Sakyo-ku, Kyoto 606, Japan. Received September 2, 1988;
Revised Manuscript Received August 7, 1989

ABSTRACT: A diaphragmatic procedure, in which a supporting film (Nafion) was put between pyrrole monomer and oxidant solution chambers, gave conducting polypyrrole-Nafion composite films through chemical polymerization of pyrrole. Two types of composite films were obtained with respect to the polarity of the adopted oxidants. One was the asymmetrical conducting composite film in the case of an anionic $\text{S}_2\text{O}_8^{2-}$ oxidant. The anionic oxidant scarcely penetrated into the Nafion owing to the Donnan exclusion effect of the fixed negative charge in the Nafion. Pyrrole permeating the Nafion was polymerized only in the oxidant side of the Nafion. The oxidant side of the resulting composite film was conducting, while its monomer side was insulating. The other showed considerable conductivity at both the oxidant side and the monomer side, when a cationic Fe^{3+} oxidant was used.

Introduction

Polypyrrole (PPy) $^{1-6}$ and its analogues, of great interest as a new type of polymer material, have been stud-

ied widely in the field of pure and applied material science. PPy has applications in such equipment as electronic devices, 7,8 electrochromic displays, $^{9-11}$ polymer batteries, $^{12-15}$ polymer-modified electrodes, 16 functional